Guidelines To Creating a True Molecular Composite: Inducing Miscibility in Blends by Optimizing Intermolecular Hydrogen Bonding

Sriram Viswanathan and Mark D. Dadmun*

Department of Chemistry, The University of Tennessee at Knoxville, Knoxville, Tennessee 37996

Received June 18, 2001

ABSTRACT: Blending a liquid crystalline polymer (LCP) with an amorphous polymer to create a molecular composite offers a method to utilize the desirable properties of a LCP at a more modest cost. However, very few such blends are miscible. In this paper, we describe the results of a study that seeks to correlate the extent of intermolecular hydrogen bonding between two polymers in a blend to its phase behavior. Using FT-IR to quantify the amount of intermolecular hydrogen bonding between the two polymers and DSC and optical microscopy to determine the phase behavior of these blends, the results demonstrate that the broadest miscibility window in the blends studied corresponds to the system that optimizes the extent of intermolecular hydrogen bonding. Moreover, the system that maximizes the extent of intermolecular hydrogen bonding is one where the hydrogen-bonding moieties on one of the polymers are separated out along the chain. These results therefore provide guidelines by which miscibility may be induced in polymer blends by the minor structural modification of one of the polymers.

Introduction

Liquid crystalline polymers (LCP) are an important class of materials with unique and desirable properties. These mesogenic fluids exhibit highly efficient molecular orientation in flow, display exceptional tensile properties, and possess viscosities lower than that of conventional polymers of comparable molecular weight. LCPs have thus been found to have potential applications as high-strength fibers and plastics.[1−5] However, the high cost of LCPs has kindled interest in many[6−12] to investigate the feasibility of blending them with commodity amorphous polymers and thereby forming rigid rod/flexible coil polymer blends that ideally would exhibit extraordinary mechanical properties and processability. Such a miscible polymer blend containing a rigid rod polymer and an amorphous coiled polymer is often termed a "molecular composite" as the rodlike polymer will act as a reinforcing "filler" of the coiled polymer with a high aspect ratio *if* the rodlike polymer is molecularly dispersed in the amorphous matrix.

Unfortunately, this is not usually the case when mixing a rodlike polymer and an amorphous polymer as most polymer pairs are incompatible and form two phases when mixed.[13] This is primarily due to the inherently low entropy of mixing two long polymer chains and the fact that the enthalpy of mixing is often a positive quantity. This immiscibility leads to a sample with poor mechanical properties due to the presence of a weak biphasic interface in the blend. To form a miscible polymer blend, the change in the Gibbs free energy of mixing (ΔG_m) on mixing the two components must be negative and the second derivative of ΔG_m with respect to the blend composition must be positive. The simplest theoretical model that provides an analytical expression for the change in the Gibbs free energy upon mixing two dissimilar polymers is the Flory−Huggins theory[13] which expresses ΔG_m as

$$\frac{\Delta G_m}{RT} = \frac{\Phi_A}{M_A} \ln \Phi_A + \frac{\Phi_B}{M_B} \ln \Phi_B + \chi_{AB}\Phi_A\Phi_B$$

where Φ_A and Φ_B and M_A and M_B are the volume fractions and degrees of polymerization of polymers A and B, respectively. The first two terms correspond to the contribution to the free energy of mixing from combinatorial entropy and becomes vanishingly small for polymer−polymer mixtures.[14,15] The third term denotes the change in enthalpy of mixing, whose sign is determined by the Flory interaction parameter χ_{AB}. In the presence of dispersive forces, the value of χ_{AB} usually tends to be significantly positive, thus resulting in most mixtures of two polymers being phase separated. A particular assumption of the Flory−Huggins theory that is relevant to this work is that the two polymers mix randomly.[16,17] This assumption does not hold in the presence of intermolecular interactions such as hydrogen bonding, due to the fact that strong intermolecular interactions will limit the mobility of polymer chains and may force polymer chains in to nonrandom configurations.

In addition to the above considerations, when one of the polymers in the mixture is a rigid rod and the other one is a random coil, the tendency of the mixture to phase separate is further intensified. Flory has shown that a rod/coil polymer blend dissolved in a solvent will separate into an isotropic phase which consists mainly of a coiled polymer solution and an anisotropic phase which consists mainly of the rodlike polymer.[16] The structural similarity of the rodlike chains provides an impetus for them to align relative to each other and exclude a structurally dissimilar coillike chain. This tendency governs the phase behavior/miscibility behavior of most rod/coil mixtures.[16]

Therefore, thermodynamics indicates that rods and coils do not want to mix; however it is economically desirable to create a molecular composite, i.e., a miscible blend containing a liquid crystalline polymer and an amorphous polymer. Fortunately, the formation of strong specific interactions between two polymers may enhance their miscibility. This makes polymer blends that allow strong intermolecular interactions an important and well-studied class of polymer blends. The presence of strong specific intermolecular interactions, such as hydrogen bonding, between two polymer chains may induce miscibility by creating sufficient favorable

10.1021/ma011031x CCC: $22.00
Published on Web 05/15/2002

enthalpic interactions to result in a negative free energy of mixing. Painter and co-workers[18−20] have studied this phenomenon extensively and have developed a theory to describe the thermodynamics of mixing two polymers that possess functional groups capable of strong intermolecular interactions such as hydrogen bonding. They write the theoretical expression for the change in free energy upon mixing as

$$\frac{\Delta G_m}{RT} = \frac{\Phi_A}{M_A} \ln \Phi_A + \frac{\Phi_B}{M_B} \ln \Phi_B + \chi_{AB}\Phi_A\Phi_B + \frac{\Delta G_H}{RT}$$

where Φ_A, Φ_B, M_A, M_B, and χ_{AB} have the same definitions as in the original Flory−Huggins theory. This equation consists of the standard combinatorial entropy (first two terms) and the unfavorable "physical" interactions represented by χ_{AB}; however, it also incorporates a third contribution (ΔG_H) that accounts for the change of entropy and enthalpy that derives from the presence of strong intermolecular interactions.

Strong, specific interactions bring about an obvious favorable change in enthalpy but also tend to produce strong orientational effects and thus decrease the entropy of mixing. Thus, the change in the enthalpy and *entropy* of the system due to the presence of strong intermolecular interactions must be accounted for. To account for the enthalpic contributions to the free energy of mixing, corresponding to both self- and intermolecular associations, and the entropic changes corresponding to loss of rotational freedom due to specific interactions, Painter et al.[18,21] have developed an association model that correlates ΔG_H to the change in the number of hydrogen-bonded species with concentration and temperature. This model accounts for the fact that hydrogen bonds are in a state of dynamic equilibrium and thus exist as a distribution of free (non-hydrogen-bonded) and hydrogen-bonded species at any instant at a given temperature and therefore must be characterized by a suitable equilibrium constant.

Thus, the formation of intermolecular hydrogen bonds between two polymers in a blend plays an integral role in its miscibility, and therefore, the extent of intermolecular hydrogen bonds that can occur between two polymers is an important parameter in determining the thermodynamics of such blends. Moreover, there are many parameters that impact the extent of intermolecular hydrogen bonding that can exist between two polymers. For instance, if one polymer can undergo intramolecular hydrogen bonding with itself, then the presence of this intramolecular hydrogen bonding will limit the amount of hydrogen-bonding moieties that are available to participate in intermolecular hydrogen bonding. Intramolecular hydrogen bonding that occurs between similar polymer chains in a polymer blend is not the only factor that can impact the extent of intermolecular hydrogen bonding. The accessibility of functional groups that participate in intermolecular interactions also plays an important role in the formation of interchain contacts. For example, factors such as steric shielding of the functional moieties due to the presence of neighboring bulky groups or steric crowding of hydrogen-bonding groups due to limited spacing between functional groups in a chain can inhibit the ability of functional groups to form specific interactions with other chains. Coleman and Painter have shown how such factors affect the accessibility of functional groups to interact between different chains by correlating the extent of interchain contacts to steric accessibility of a hydrogen-bonding functional group and spacing between functional groups in a polymer chain. More specifically, they monitored the extent of intermolecular hydrogen bonding that can occur in a variety of blends consisting of a wide range of carbonyl-containing (co)polymers and hydroxyl-containing (co)polymers. As an example, they studied blends containing poly(*n*-alkyl methacrylate) (PAMA) having different side chain lengths and poly(2,3-dimethylbutadiene-*stat*-4-vinylphenol) (DMBVPh) containing 24 wt % VPh.[22] This study shows that steric shielding of the carbonyl due to the *n*-alkyl side chain decreases the intermolecular interactions. Using the interassociation equilibrium constant (K_A) as an indicator of intermolecular hydrogen bonding, they have shown that a decrease in the side chain length in the PAMA results in an increase in K_A, which correlates to an increase in intermolecular hydrogen bonding. In these studies, the poly(*n*-alkyl methacrylates) poly(methyl methacrylate) (PMMA), poly(ethyl methacrylate) (PEMA), poly(*n*-butyl methacrylate) (PBMA), poly(*n*-hexyl methacrylate) (PHMA), poly(*n*-decyl methacrylate) (PDMA), and poly(*n*-lauryl methacrylate) (PLMA) were examined.

In another set of experiments, Coleman and Painter examined blends of PAMA and DMBVPh with various copolymer compositions (24, 48, and 72 wt % VPh).[22] This study elucidated the effect of spacing the hydroxyl groups in the DMBVPh chain on the amount of intermolecular H-bonding that occurs in these blends. Their experiments showed an increase in interchain H-bonding as the amount of VPh was decreased from 72 to 24 wt % in DMBVPh (and thus increased the spacing between the −OH groups on the chain), regardless of the steric shielding in PAMA. The authors interpreted these results as evidence that the spacing of hydroxyl groups on a copolymer chain can dramatically affect the amount of intermolecular H bonding in polymer blends. They attribute this trend to the fact that spacing hydroxyl groups apart allows these groups to rotate independently with respect to one another, thus allowing them to reorient themselves in such a way that they are readily available for hydrogen bonding. However, the spacing effect does not provide any further increase in interchain H bonding below 24 wt % VPh, as the number of VPh groups in the copolymer becomes so low as to limit the number of possible intermolecular H bonds that can be formed.

Further experiments by Coleman et al. provide further evidence of the importance of spacing groups along the chain on the extent of intermolecular hydrogen bonding by examining blends that contain DMBVPh and poly(ethylene-*co*-vinyl acetate) (EVAc).[23] These results show an increased accessibility of the VAc carbonyl groups to form interchain H bonds as the spacing between the carbonyl groups in EVAc increases. This trend continues until 18 wt % VAc in EVA, below which there is a decrease in interchain H bonding, due to a decrease in the possible number of H bonds that can be formed. Coleman and Painter have also studied other systems to examine the effect of functional group spacing and steric crowding on the extent of intermolecular hydrogen bonding. Each of these studies has shown that an increased spacing between functional groups on a chain increases the amount of intermolecular hydrogen bonding; however, the optimum spacing seems to be system dependent.[24,25] These results also verify that

Table 1. Molecular Weights and Phase Transitions of LCPU and PS-*co*-VPh Copolymers[a]

	mol wt (g/mol)		phase transition temp (°C)		
polymer	M_n	M_w	T_g	T_m	T_i
LCPU	35 000	53 600	87	132	160
PS-*co*-VPh(5)	13 700	21 300	101		
PS-*co*-VPh(10)	20 700	34 500	103		
PS-*co*-VPh(20)	47 100	90 100	105		
PS-*co*-VPh(30)	22 100	32 400	108		
PS-*co*-VPh(40)	31 300	61 100	114		
PS-*co*-VPh(50)	34 100	65 200	116		
PVPh	22 000		147		

[a] T_m = crystalline melt temperature, and T_i = nematic to isotropic transition temperature.

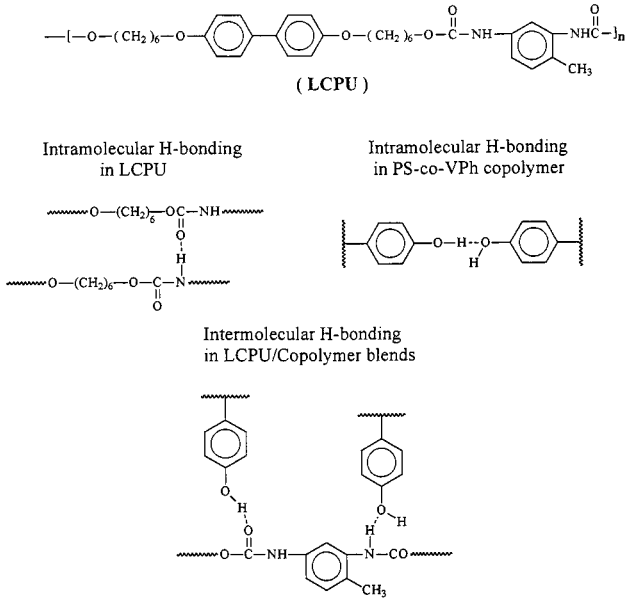

Figure 1. Structure of the liquid crystalline polyurethane (LCPU) used in this study as well as possible hydrogen-bonding associations in blends containing the LCPU and a copolymer of styrene and vinylphenol (PS-*co*-VPh).

steric crowding can limit access of functional groups to participate in intermolecular hydrogen bonding.

Elsewhere, Radmard et al.[26] have studied the effect of functional group spacing along a polymer chain on the amount of intermolecular H bonding that forms between a rigid and a flexible polymer. They studied a blend containing a rigid liquid crystalline polyether (DHMS-7,9) and flexible poly(styrene-*co*-4-vinylphenol) (PS-*co*-VPh). An increase in the amount of intermolecular hydrogen bonding as the amount of VPh in the PS-*co*-VPh decreases (and the spacing of the −OH groups increases) is observed in blends that consist of DHMS-7,9 and PS-*co*-VPh copolymers that contain 10, 20, and 100 mol % VPh. Their results are in agreement with those of Coleman and Painter, indicating that, even for systems with chains that differ in stiffness, spacing the hydroxyl groups apart on the copolymer chain produces a significant amount of, and may optimize the extent of, intermolecular H bonding.

Coleman and Painter have also identified another important factor that affects the formation of intermolecular interactions. A flexible chain can bend back upon itself to avoid intermolecular interactions, thus inhibiting the formation of intermolecular interactions. This effect has been termed intramolecular screening. Coleman et al. have developed a method to account for this effect by correlating the screening effect caused by intrachain contacts to chain connectivity and chain flexibility.[27,28] By introducing this screening parameter γ, they have shown improved agreement between theoretical and experimental phase diagrams relative to theoretical calculations that do not include the screening parameter. For example, their studies on blends containing poly(ethyl methacrylate-*stat*-4-vinylphenol) (EMAVPh, 55 wt % VPh) and poly(ethylene oxide) (PEO) show a larger disparity between the theoretical and experimental phase diagrams when the screening parameter is excluded from theoretical estimations than when it is included.[28] They have obtained similar results examining EMAVPh blends with poly(ethylene oxide-

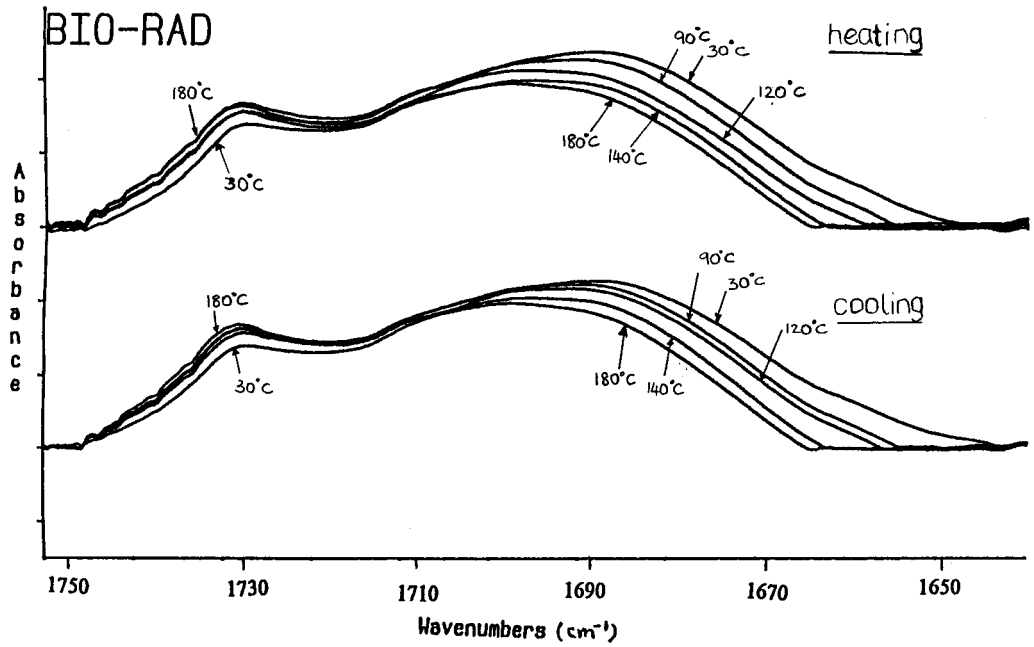

Figure 2. Representative FT-IR spectra of C═O stretching region for pure LCPU as a function of temperature during heating and cooling cycles.

stat-propylene oxide) copolymer. A recent work by Coleman and Painter has also examined the intramolecular screening effect in systems containing dendrimers.[29] They have shown that intramolecular screening is less significant in hyperbranched polyesters with 2 generations than it is in hyperbranched polyesters with 5 generations.

Thus, polymer blends containing a liquid crystalline polymer and an amorphous polymer will have a propensity to phase separate, but sufficient hydrogen bonding between two immiscible polymers may induce miscibility. Moreover, there exist a significant number of parameters that can be manipulated to optimize the extent of intermolecular hydrogen bonding and thus the phase behavior of these mixtures. Therefore, in the quest to design and create a molecular composite reproducibly, an understanding of the relationship between these controllable parameters, the extent of intermolecular hydrogen bonding, *and* the phase behavior of the mixtures containing an amorphous polymer and a LCP must be more clearly understood. Is it possible to form a miscible blend containing a LCP (rodlike) and an amorphous polymer (coillike) by incorporating hydrogen bonding between the two components? If so, under what conditions might this be feasible? Previously, Painter et al.[8,30] and Green et al.[31] have shown that a thermodynamically stable molecular composite can be found by incorporating hydrogen bonding between the LCP and amorphous polymer. However, a detailed study has not been attempted to provide guidelines by which miscible blends of LCP and amorphous polymers may be *designed* and created. Clearly, there should be a correlation between the extent of hydrogen bonding between two polymers and the phase behavior of their blend. This paper presents data and experimental results that make this correlation.

More specifically, a blend containing a liquid crystalline polyurethane and an amorphous copolymer that contains a monomer that can participate in hydrogen bonding (vinylphenol, VPh) and one that cannot (styrene) has been examined. FT-IR has been used to determine the extent of intermolecular hydrogen bonding that occurs in the blend as a function of the spacing of the hydrogen-bonding functional groups (as controlled by the composition of the copolymer). This parameter will then be correlated to the phase behavior of the blends.

Therefore, this paper will present results that will elucidate the effect of the composition of the amorphous copolymer that contains a non-hydrogen-bonding and a hydrogen-bonding monomer on the extent of intermolecular hydrogen bonding of a blend containing this copolymer and a liquid crystalline polymer. These data will then be related to the phase behavior of the blends to illustrate the correlation between the extent of intermolecular hydrogen bonding and blend miscibility of a molecular composite and provide guidelines by which these materials can be designed and produced.

Experimental Section

Materials. 4,4-Biphenol and 2,4-toluene diisocyanate (TDI) were obtained from TCI America Inc., styrene, 4-acetoxystyrene, and hydrazine hydrate were purchased from Aldrich Chemical Co., azobis(isobutyronitrile) (AIBN) was purchased from Dojac Inc., and sodium hydroxide, 6-chlorohexanol, methanol, dioxane, *N,N′*-dimethylformamide (DMF), and 1-butanol were purchased from Fisher-Acros. Poly(4-vinylphenol) (PVPh) was purchased from Polysciences Inc. In the polymerization of the liquid crystalline polyurethane (LCPU), DMF, 1-butanol, and TDI were purified by vacuum distillation before use. All other chemicals were used as received.

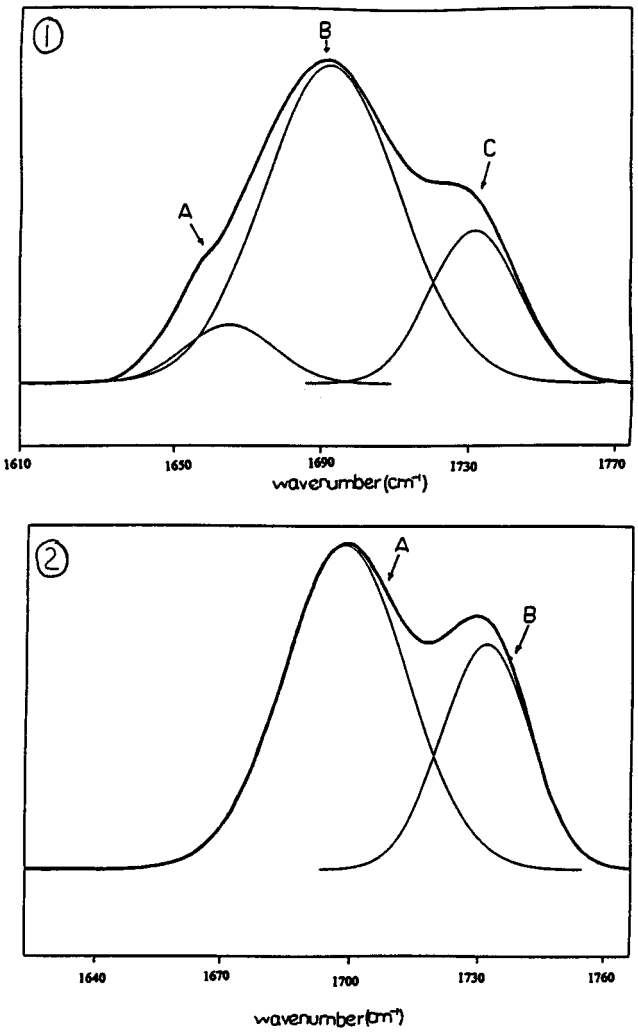

Figure 3. Example of curve-fitting procedure in the carbonyl stretching regime of FT-IR spectra of the pure LCPU measured at (1) 30 °C (upon cooling) and (2) 180 °C.

Experimental Techniques. Molecular weights of the synthesized polymers were determined using a Waters gel permeation chromatograph equipped with Ultrastyragel columns with a refractive index detector. DMF was used as elution solvent for the LCPU and tetrahydrofuran (THF) for the styrenic copolymers (PS-*co*-VPh). Narrowly dispersed polystyrene was used as calibration standard for both. Differential scanning calorimetry (DSC) measurements were completed to determine thermal properties of the polymers and blends and were run at 10 °C/min using a Mettler DSC 821 calibrated with indium.

Structure and compositions of the LCPU and PS-*co*-VPh copolymers were determined by proton NMR spectroscopy on a 250 MHz Bruker NMR using TMS as an internal standard. The solvents for these NMR experiments were deuterated dimethyl sulfoxide for the LCPU and deuterated chloroform for the PS-*co*-VPh copolymers.

Infrared spectra were obtained on a Biorad FTS-60A Fourier transform infrared (FT-IR) spectrometer purged with dried air using a minimum of 64 scans at a resolution of 2 cm^{-1}. The frequency scale was internally calibrated with a He−Ne reference to an accuracy of 0.2 cm^{-1} and externally with polystyrene. Samples for FT-IR studies were obtained by solvent-casting blends of LCPU and PS-*co*-VPh from DMF (2% w/v) on KBr disks at room temperature. The KBr disks were placed on a horizontal holder in a desiccator to reduce the

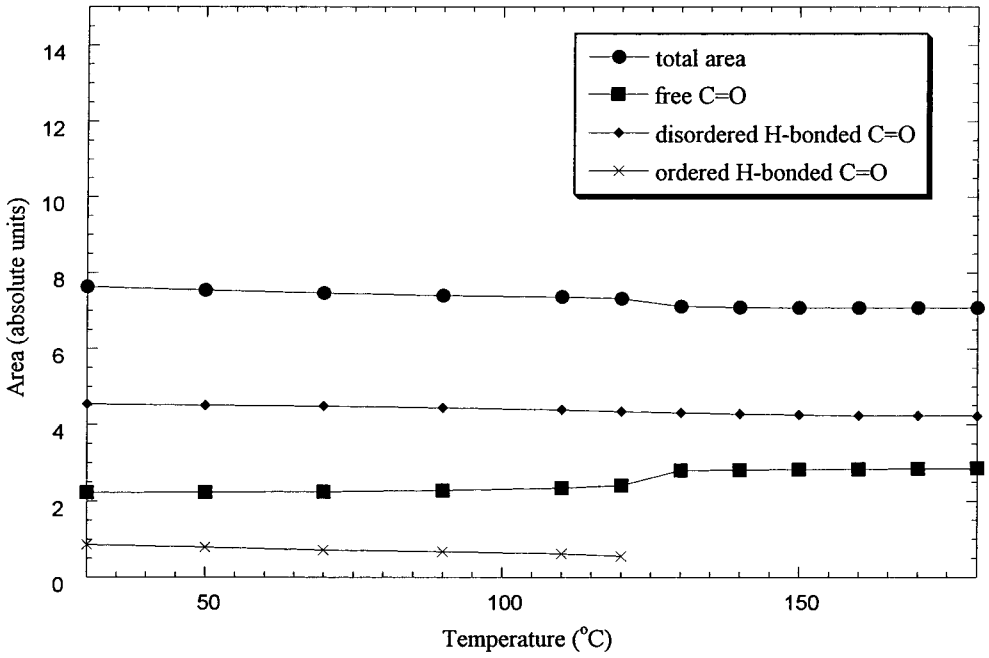

Figure 4. Plot of peak areas from curve fitting of C═O stretching band of the pure LCPU FT-IR spectra as a function of temperature as the sample is cooled from 180 to 30 °C.

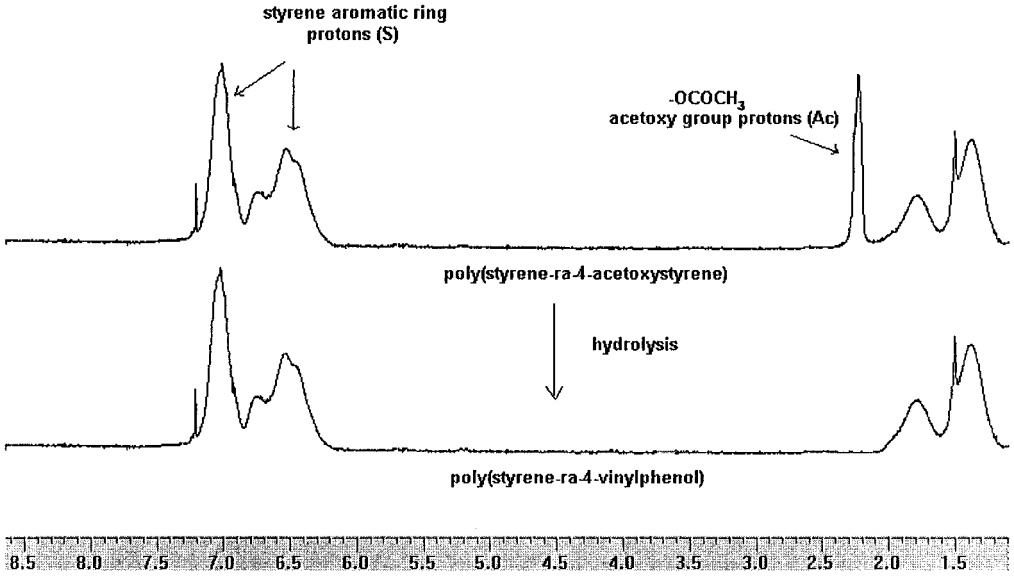

Figure 5. Characteristic ^{1}H NMR spectra of poly(styrene-*ra*-4-acetoxystyrene) and poly(styrene-*ra*-4-vinylphenol).

evaporation rate and to avoid film cracking. After evaporating most of the solvent at room temperature, the disks were subsequently dried in a vacuum oven at 60 °C for 3 days to remove residual solvent and moisture. The absence of solvent in the sample was verified by the absence of the C═O peak of DMF which occurs at 1650 cm^{-1} in the IR curve, which occurs at a lower wavenumber than the C═O peak of the LCPU (1730 cm^{-1}). The films prepared for FTIR were adequately thin to be within an absorbance range where the Beer−Lambert law is satisfied. High-temperature spectra were obtained using a cell mounted in the spectrometer connected to a temperature controller. The temperature was controlled to an accuracy of 0.5 °C. For high-temperature experiments, the temperature was maintained constant for 15 min at a given temperature before running the scans to ensure that the sample had reached thermal equilibrium.

Phase behavior data of the blends were obtained by preparing 2% (w/v) solutions of the blend in DMF and spotting them on a microscope slide. The solvent was allowed to evaporate in a desiccator first and then overnight in a vacuum oven at 60 °C to remove residual solvent. The phase behavior of the blends was monitored by phase contrast and polarized optical microscopy using an Olympus BH-2 optical microscope equipped with a Mettler FP82HT hot stage.

Polymer Synthesis. The liquid crystalline polyurethane was synthesized by the condensation of 4,4′-bis(6-hydroxyhexoxy)biphenyl (BHHBP) and 2,4-toluene diisocyanate (TDI) according to literature procedures.[32] BHHBP was also prepared according to literature procedures via the condensation of 4,4-biphenol with 6-chlorohexanol.

Poly(styrene-*co*-4-vinylphenol) (PS-*co*-VPh) random copolymers were prepared by the free radical polymerization of styrene and 4-acetoxystyrene using AIBN as the initiator followed by the hydrolysis of the acetoxy groups using hydrazine hydrate according to the procedure of Green and Khatri.[31] Copolymers containing 5, 10, 20, 30, 40, and 50 mol % vinylphenol were synthesized and utilized in this study. Hereinafter, PS-*co*-VPh(*n*) denotes a PS-*co*-VPh copolymer with *n* mol % VPh. The molecular weight characteristics and thermal behavior of these polymers are listed in Table 1.

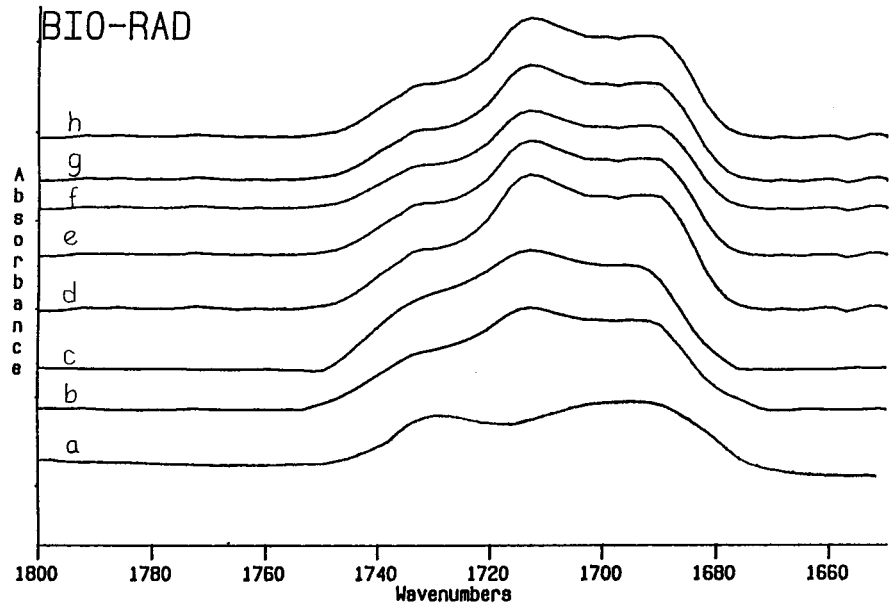

Figure 6. FT-IR spectra of C═O stretching region for blends measured at 180 °C. Compositions of blends are 80 wt % PS-*co*-VPh and 20 wt % LCPU. Curve (a) is the pure LCPU, while the remaining curves are for blends containing PS-*co*-VPh with (b) 5, (c) 10, (d) 20, (e) 30, (f) 40, (g) 50, and (h) 100 mol % VPh.

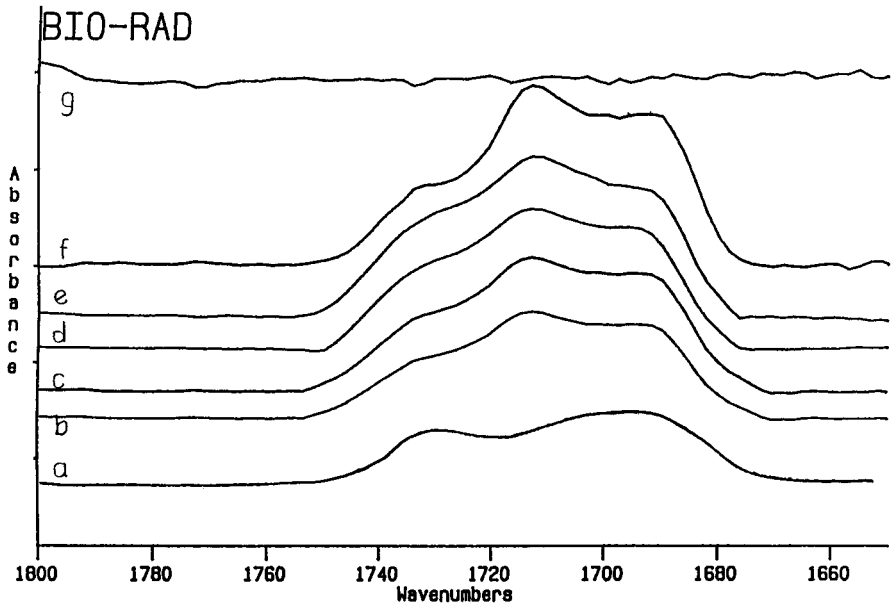

Figure 7. FT-IR spectra of C═O stretching region for blends containing PS-*co*-VPh(20) measured at 180 °C. The curves correspond to blends with a composition of (LCPU/PS-*co*-VPh wt/wt) (a) 100/0, (b) 80/20, (c) 60/40, (d) 50/50, (e) 40/60, (f) 20/80, and (g) 0/100.

Results and Discussion

The aim of this study is to understand the correlation between the copolymer composition, the extent of intermolecular hydrogen in a blend containing a liquid crystalline polymer and an amorphous copolymer, and the phase behavior of that blend. The structure of the LCPU and the scheme of hydrogen bonding in LCPU/PS-*co*-VPh blends are shown in Figure 1. To determine the amount of intermolecular H bonding between the two blend components, FT-IR was used to evaluate the carbonyl stretching vibration around 1700 cm^{-1}. The curve fitting of the absorbance IR peaks was performed by Peakfit software version 3.0 with baseline correction. It is well-known that the C═O bond strength decreases upon hydrogen bonding.

To interpret the curve-fitting peaks that comprise the C═O stretching band of the LCPU/PS-*co*-VPh blends, a prior understanding of the C═O stretching band of the pure LCPU is required. Analysis of the C═O stretching band of pure LCPU at 30 °C reveals three peaks that are assigned to free C═O groups (around 1730 cm^{-1}), C═O groups that are intramolecularly hydrogen bonded to N−H that are disordered (around 1690 cm^{-1}), and ordered hydrogen-bonded C═O groups (to N−H groups) (around 1670 cm^{-1}). The assignment of these peaks was completed by interpretation of their temperature dependence and the correlation of this behavior to previous hydrogen-bonding studies of polyurethanes.[33] Thus, temperature studies of the pure LCPU and its blends were carried out from 30 to 180 °C (heating cycle) and back to 30 °C (cooling cycle). Representative IR curves on heating and cooling cycles for the pure LCPU are shown in Figure 2. These curves were then fit to obtain the area under the three peaks,

Table 2. Results of the Curve Fitting to the C═O Stretching Region for Pure LCPU and Blends Containing 80 wt % PS-*co*-VPh Copolymer for Various Copolymer Compositions Measured at 180 °C

% VPh in PS-*co*-VPh	free C═O			intermolecularly H-bonded C═O			interamolecularly H-bonded C═O			% C═O intermolecularly H-bonded
	υ,[a] cm^{-1}	$W_{1/2}$, cm^{-1}	A_1	υ, cm^{-1}	$W_{1/2}$, cm^{-1}	A_2	υ, cm^{-1}	$W_{1/2}$, cm^{-1}	A_1	
pure LCPU	1732	24.0	2.854				1695.4	32.1	4.225	
5	1732	22.8	2.152	1714.8	23.7	0.967	1694.9	27.7	3.880	11.96
10	1732	23.5	2.023	1714.3	24.0	1.703	1695.5	25.4	3.837	19.69
20	1732	23.2	1.426	1713.7	24.8	2.845	1694.4	24.2	3.090	25.00
30	1732	22.7	1.493	1713.7	24.6	3.096	1694.7	24.5	3.181	36.10
40	1732	12.1	1.493	1713.6	24.5	3.161	1694.9	23.9	3.213	36.50
50	1732	22.9	1.356	1713.5	24.7	2.972	1694.6	24.2	2.970	37.00
100	1732	22.5	1.373	1713.5	24.8	3.075	1694.9	23.7	3.100	37.10

[a] Fixed during curve fitting. Absorptivity coefficient (K) = 1.54; $A_2' = A_2/K$; $A_3' = A_3/K$; $A_T = A_1 + A_2' + A_3'$; % C═O intermolecularly H-bonded = $(A_2'/A_T) \times 100$.

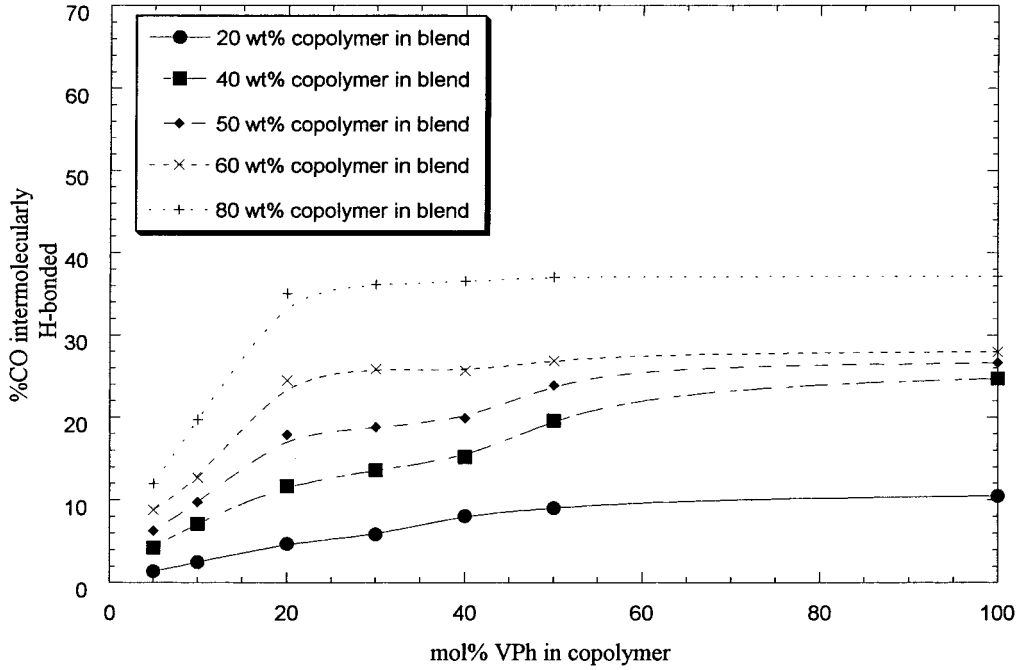

Figure 8. Change in the percent of carbonyl groups participating in intermolecularly hydrogen bonding as a function of PS-*co*-VPh copolymer composition for different blend compositions.

as shown in Figure 3a, which shows the analysis for the sample at 30 °C. The fitting shown in Figure 3b is for the LCPU at 180 °C, where only two peaks exist. It is clear from these figures that the peak at 1670 cm^{-1}, associated with the ordered (crystalline) hydrogen-bonded C═O, has disappeared at 180 °C. This is expected as the LCPU melts at 130 °C. Figure 4 shows the temperature dependence of the areas under each of the three peaks, corroborating the assignment of the three initial peaks in the neat LCPU IR curve. As the temperature increases, there is an increase in the free C═O peak, a slight decrease in the disordered H-bonded C═O peak, and a decrease and abrupt disappearance of the ordered H-bonded C═O peak at 130 °C. The cooling cycle shows a reverse trend except that the ordered H-bonded component appears at 120 °C.

Once the IR peaks associated with the LCPU have been clarified, the hydrogen-bonding behavior of the blends can be accurately examined. Thus, the C═O band in the LCPU/PS-*co*-VPh blends were monitored and curve fitted as a function of temperature, blend composition, and PS-*co*-VPh composition. The IR curves of the blends were examined at a series of temperatures ranging from room temperature to 180 °C. While there is very little difference in the trends described below with temperature, the data at 180 °C (above the T_g and T_m of all blend components) are reported to ensure that ordering of the LCP does not influence the results and that the samples were allowed to reach equilibrium. The IR curves for the blends near the C═O stretching regime show three peaks that are assigned to free (non-hydrogen-bonded) carbonyl groups [around 1730 cm^{-1}], intermolecularly hydrogen-bonded C═O groups (to O−H groups) [around 1715 cm^{-1}], and (disordered) intramolecularly hydrogen-bonded C═O groups (to N−H groups) [around 1690 cm^{-1}]. Analysis of these peaks provides a mechanism to determine the percentage of carbonyl groups in the system that participate in intermolecular hydrogen bonding.[18] However, the percentage of hydroxyl groups on the styrenic copolymer that intermolecularly hydrogen bond to the LCPU cannot be quantitatively determined by curve fitting the O−H stretching band at 3300 cm^{-1}. This is primarily due to the presence of overlap between the N−H stretching and O−H stretching bands. Additionally, the presence of the overtone of the fundamental C═O stretching vibration in this region provides additional difficulties in analyzing this region of the IR spectra.[33] Therefore, the amount of OH that is participating in intermolecular hydrogen bonding is determined stoichiometrically. The number of carbonyl and hydroxyl units in the blend is estimated from the composition and molecular weights

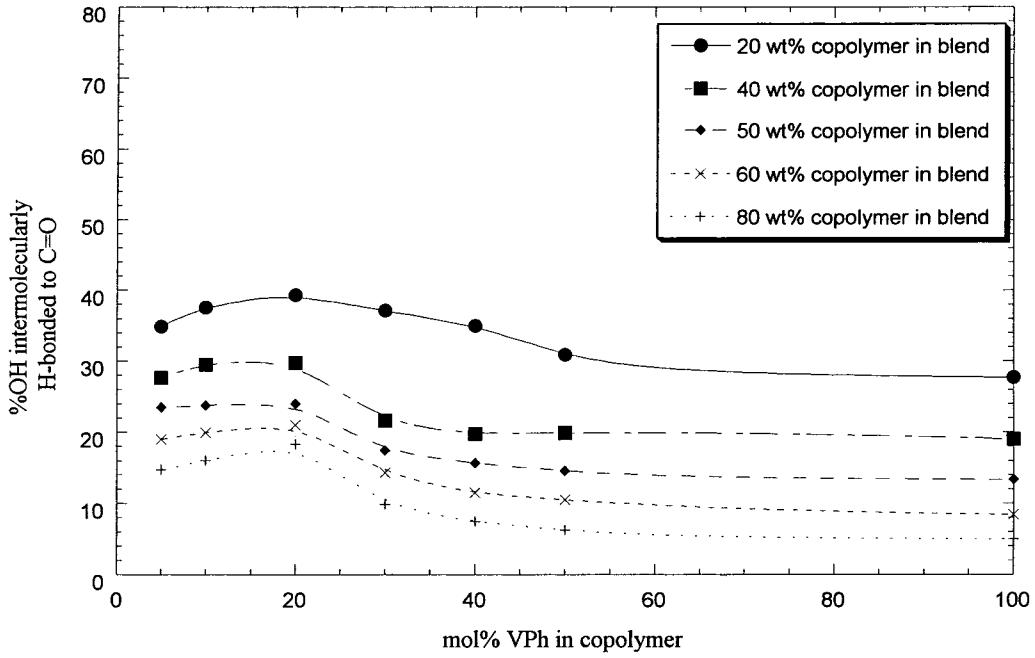

Figure 9. Change in the percent of hydroxyl groups participating in intermolecularly hydrogen bonding as a function of PS-*co*-VPh copolymer composition for different blend compositions.

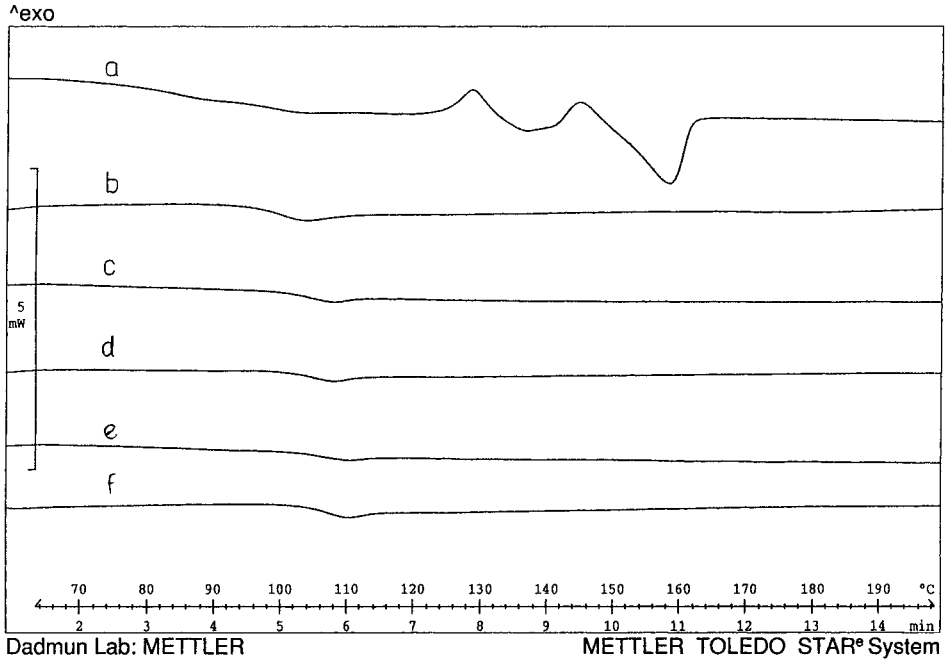

Figure 10. Representative DSC curves of blends containing LCPU and PS-*co*-VPh(10). Compositions of the blends are (LCPU/PS-*co*-VPh(10) wt/wt) (a) 25/75, (b) 20/80, (c) 15/85, (d) 10/90, (e) 5/95, and (f) 0/100.

of the two polymers, and the percentage of hydroxyl groups that participate in intermolecular hydrogen bonding is then estimated by dividing the percentage of carbonyl groups participating in hydrogen bonding by the ratio of the number of hydroxyl groups to carbonyl groups present in the blend. This procedure is shown mathematically as

$$\Gamma(\mathrm{OH}) = \Gamma(\mathrm{C{=}O})/(N_{\mathrm{OH}}/N_{\mathrm{C=O}})$$

where Γ(OH) is the percentage of hydroxyl groups that are participating in intermolecular hydrogen bonding, Γ(C=O) is the percentage of carbonyl groups that are participating in intermolecular hydrogen bonding, N_{OH} is the total number of hydroxyl groups present in the blend, and $N_{\mathrm{C=O}}$ is the total number of carbonyl groups present in the blend.

The composition of the PS-*co*-VPh copolymer is determined by integration of NMR spectra, as shown in Figure 5, using the method of Radmard[34] and Coleman and Painter.[35] In this procedure, the area for the methyl group in the acetoxy moiety (ca. 2.2 ppm) is compared to the area of the aromatic hydrogens (ca. 6.2−7.2 ppm). Because each acetoxy group present will have displaced one aromatic hydrogen and corresponds to an aromatic ring with four aromatic hydrogens, it is easily shown

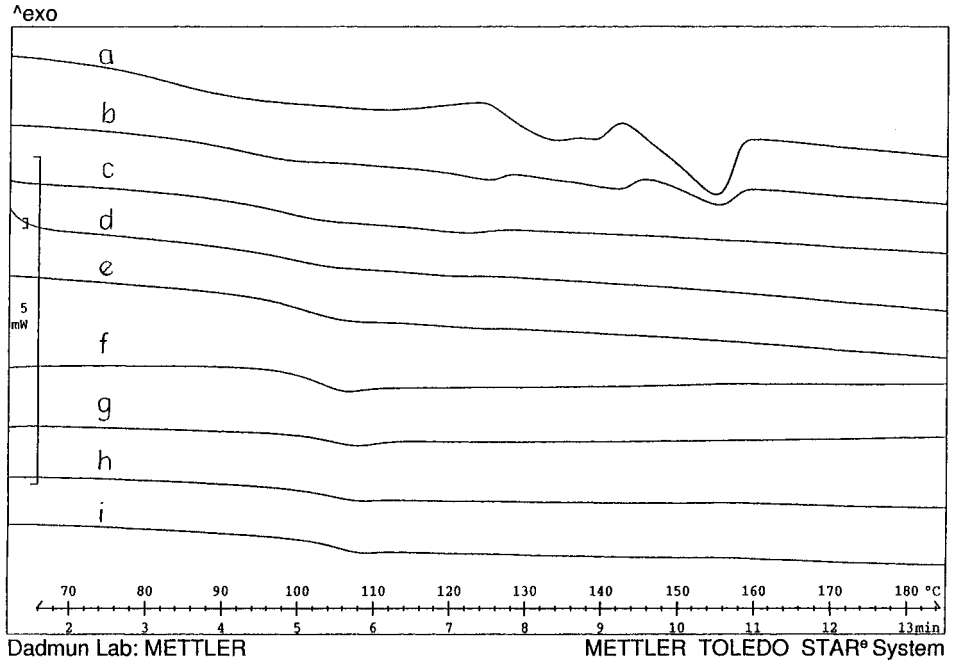

Figure 11. Representative DSC curves of blends containing LCPU and PS-*co*-VPh(20). Compositions of the blends are (LCPU/PS-*co*-VPh(20) wt/wt) (a) 40/60, (b) 35/65, (c) 30/70, (d) 25/75, (e) 20/80, (f) 15/85, (g) 10/90, (h) 5/95, and (i) 0/100.

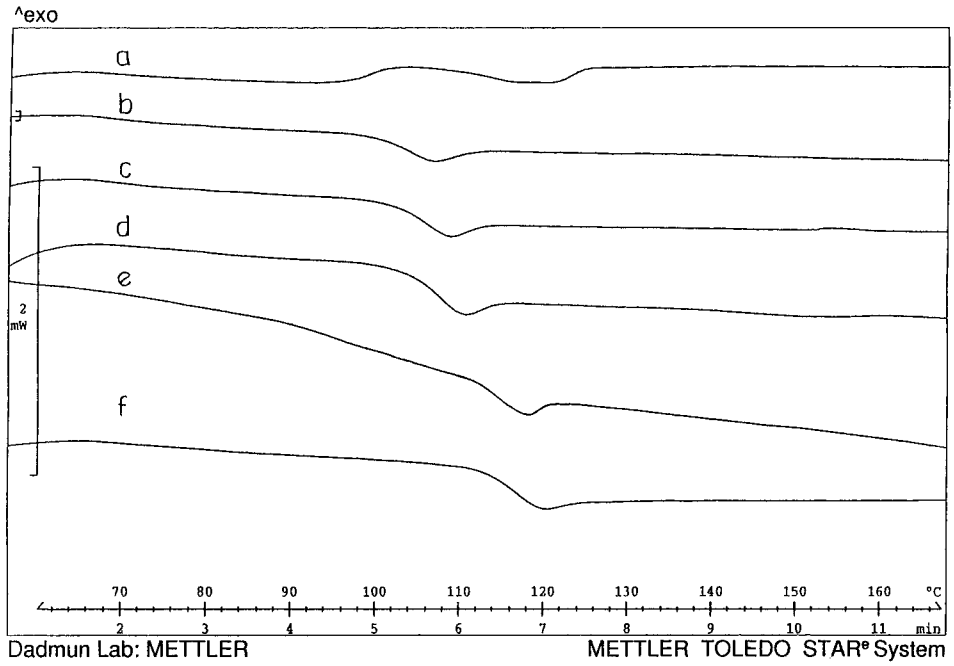

Figure 12. Representative DSC curves of blends containing LCPU and PS-*co*-VPh(30). Compositions of the blends are (LCPU/PS-*co*-VPh(30) wt/wt) (a) 25/75, (b) 20/80, (c) 15/85, (d) 10/90, (e) 5/95, and (f) 0/100.

that the composition of the copolymer is given by

$$\pi_{sty} = \frac{3A_{ar} - 4A_{me}}{3A_{ar} - A_{me}}$$

where $\pi_{sty} \times 100$ is the percent styrene in the copolymer, A_{ar} is the area under the aromatic peaks, and A_{me} is the area under the acetoxy methyl group peak.

Figure 6 shows the FT-IR curves in the C=O stretching region (1800−1650 cm^{-1}) for a blend containing PS-*co*-VPh and LCPU (20 wt % LCPU) for differing copolymer compositions measured at 180 °C. This figure illustrates that there is an increase in the amount intermolecularly hydrogen bonding as the amount of VPh in the copolymer increases from 0 to 20% (curves b−d), as is demonstrated by the increase in the carbonyl peak at 1710 cm^{-1}. However, very little change is observed in this peak above 20% VPh in the copolymer (curves e−h). FT-IR curves of the C=O stretching region of blends that contain LCPU and PS-*co*-VPh(20) of various blend compositions measured at 180 °C are shown in Figure 7. This figure shows an increase in the extent of intermolecularly H-bonded C=O groups as the amount of PS-*co*-VPh(20) in the blend increases from 0 to 80 wt %, illustrated by an increase in the peak at around 1710 cm^{-1}. A more quantitative understanding

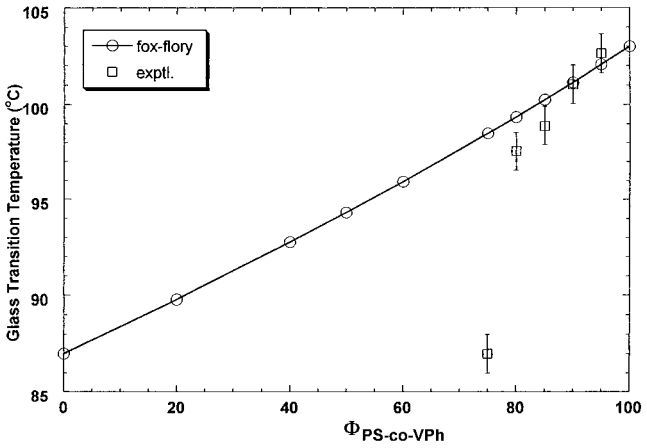

Figure 13. Experimental and theoretical glass transition temperatures of blends containing PS-*co*-VPh(10) and LCPU.

of the extent of intermolecular hydrogen bonding in these blends can be obtained by curve fitting the C═O absorbance peaks in these IR curves. Parameters obtained from the curve-fitting procedure of the C═O stretching region for the free C═O, intermolecularly H-bonded C═O, and intramolecularly H-bonded C═O bands are listed in Table 2. During curve fitting, the position of the free C═O vibration in the blend was kept fixed at the same position, whereas those of the hydrogen-bonded vibrations were allowed to vary. The hydrogen-bonded C═O peak position was allowed to deviate to account for the fact that hydrogen bond geometry distribution and strength can be a function of temperature and/or blend composition.[21,36] In all cases, a Gaussian band shape was assumed.

The fitted carbonyl stretching curves are then utilized to determine the percent of carbonyl bonds that participate in hydrogen bonds. The areas under the three peaks that contribute to this portion of the spectrum are determined from the fitting procedure; A_1 is the area of the free carbonyl peak, A_2 is the area of the peak associated with the intermolecularly hydrogen-bonded carbonyls, and A_3 is the area of the intramolecularly hydrogen-bonded carbonyls peak. It is well-known that the absorptivity coefficient of the hydrogen-bonded carbonyls is greater than that of the free carbonyls. To account for this difference in absorptivity coefficients so that the data can be correctly analyzed, a ratio of the absorptivity coefficients of these bands is required. The absorptivity coefficient ratio is estimated by using the method of Coleman and Painter,[18,33,37] which employs the following equation:

$$K = [A_{HB}{}^{T2} - A_{HB}{}^{T1}]/[A_F{}^{T1} - A_F{}^{T2}]$$

where $A_{HB}{}^{T1}$ and $A_{HB}{}^{T2}$ are hydrogen-bonded carbonyl absorption intensities at temperatures T_1 and T_2 and $A_F{}^{T1}$ and $A_F{}^{T2}$ are free C═O absorption intensities at temperatures T_1 and T_2.

The absorption intensities of the H-bonded C═O bands (A_2 and A_3) were corrected for the difference in absorptivity coefficients of the H-bonded and free C═O bands by division of their experimentally determined areas by their respective K values ($A_2' = A_2/K_1$ and $A_3' = A_3/K_2$; $K_1 = K_2 = 1.54$ in this case). Furthermore, it is important to note that, unlike the N−H stretching band which is highly sensitive to temperature, the C═O stretching band is far less sensitive to temperature. In other words, the absorptivity coefficient ratio of the H-bonded C═O band to the free C═O band in the C═O stretching mode does not differ appreciably with temperature which makes it convenient for quantitative analysis.

Finally, the percent of carbonyl groups that participate in intermolecular hydrogen bonding is then calculated by

$$\% \text{ C═O} = \frac{A_2'}{A_1 + A_2' + A_3'}$$

The results of the fitting procedures for neat LCPU and LCPU/PS-*co*-VPh blends containing 80 wt % PS-*co*-VPh copolymer for various copolymer compositions measured at 180 °C are listed in Table 2.

Figure 8 shows the results of this analysis by documenting the change in the percent of carbonyl (% C═O) groups that are intermolecularly H-bonded with the composition of the PS-*co*-VPh for various blend compositions measured at 180 °C. For each blend, as the amount of hydroxyl-containing monomer (VPh) increases up to 20 mol %, the amount of C═O that participates in intermolecular hydrogen bonding increases. However, above 20 mol % VPh, the percent of carbonyl groups that participate in intermolecular hydrogen bonding changes little. Thus, adding more hydroxyl

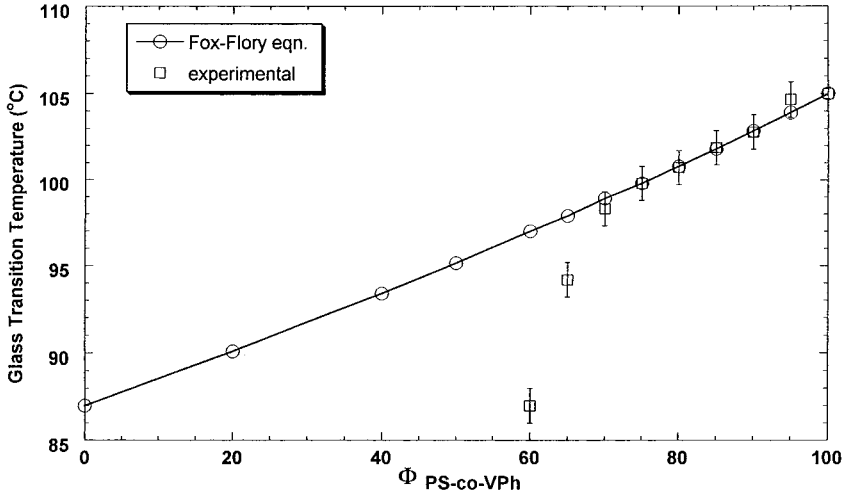

Figure 14. Experimental and theoretical glass transition temperatures of blends containing PS-*co*-VPh(20) and LCPU.

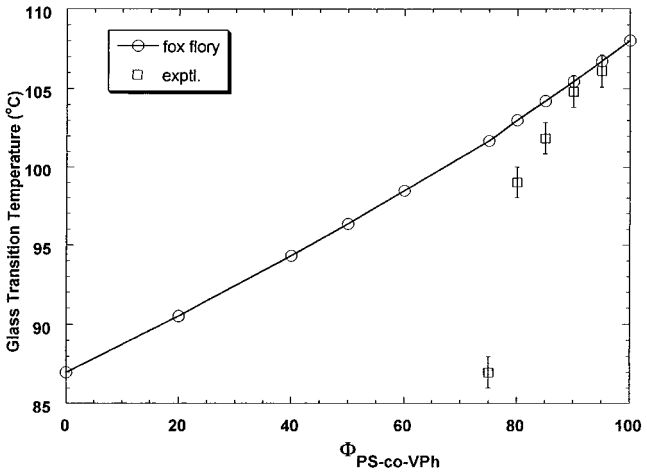

Figure 15. Experimental and theoretical glass transition temperatures of blends containing PS-*co*-VPh(30) and LCPU.

groups does not increase the extent of intermolecular hydrogen bonding above 20 mol % VPh in the copolymer. Our interpretation of this trend is that as the amount of −OH increases from 0 to 20%, more hydroxyl groups are introduced that can H-bond with C=O groups, more carbonyl groups find available −OH groups to create intermolecular hydrogen bonds, and this curve increases. However, above 20% VPh in the copolymer, the additional −O−H groups are not usually able to find suitably oriented or positioned carbonyl groups with which to form an intermolecular H-bond, and this curve remains flat. This interpretation is corroborated by examining the percentage of hydroxyl groups that participate in intermolecular H bonding with C=O. Figure 9 shows these data and demonstrates that this parameter does not change much up to 20% VPh in the copolymer but decreases as more hydroxyl groups are included on the copolymer chain. These observations indicate that when the amorphous copolymer contains 20 mol % VPh, the percent of hydroxyl groups that participate in intermolecular hydrogen bonding is maximized and the amount of carbonyl groups that engage in intermolecular hydrogen bonding is also maximized. Thus, this composition of the copolymer denotes the system where the extent of intermolecular hydrogen bonding between these two polymers is optimized. This is in agreement with the work of Radmard and coworkers, who showed that the extent of intermolecular hydrogen bonding between the two polymers with dissimilar rigidities is maximized when the hydroxyl groups along the copolymer chain are significantly separated along the chain.[26]

As mentioned earlier, the reason for this trend is related to the proximity of the hydroxyl groups on the amorphous copolymer to other hydroxyl groups. The separation of the hydroxyl groups on the chain provides each hydroxyl group with sufficient rotational freedom to enable the independent reorientation of the individual hydroxyl groups that allows more groups to orient themselves correctly near other functional groups to form intermolecular hydrogen bonding. Additionally, the separation of the hydroxyl groups along the chain also decreases the probability of forming *intra*molecular (hydroxyl to hydroxyl) hydrogen bonding.

To correlate the extent of intermolecular hydrogen bonding to the phase behavior of these blends, the phase diagrams of blends containing LCPU and copolymers that consist of 10%, 20%, and 30% VPh [PS-*co*-VPh(10), PS-*co*-VPh(20), PS-*co*-VPh(30)] were determined using DSC and optical microscopy. Figures 10, 11, and 12 show the DSC curves of LCPU/PS-*co*-VPh(10), LCPU/PS-*co*-VPh(20), and LCPU/PS-*co*-VPh(30) blends, respectively, for various blend compositions. A single glass transition of the blends is observed for blend compositions above 60 wt % PS-*co*-VPh(20) for this blend and above 80 wt % PS-*co*-VPh for the other two blend systems, suggesting miscibility of these blends in these regimes. Figure 13, 14, and 15 provide further evidence of miscibility by showing the dependence of the blend T_g (as determined by DSC) on blend composition for blends of LCPU/PS-*co*-VPh(10), LCPU/PS-*co*-VPh(20),

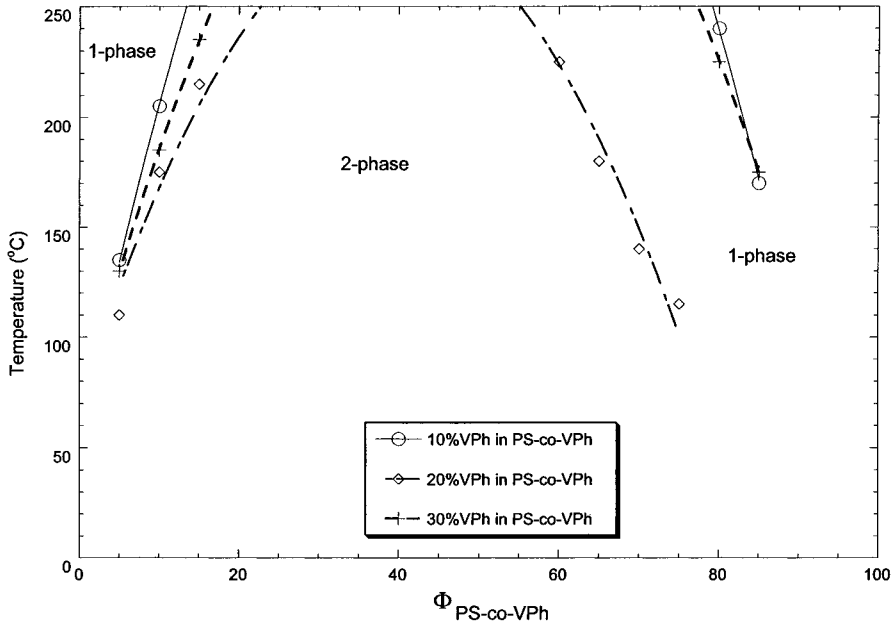

Figure 16. Phase diagram of blends containing PS-*co*-VPh(10), PS-*co*-VPh(20), and PS-*co*-VPh(30) as determined from phase contrast optical microscopy.

and LCPU/PS-*co*-VPh(30), respectively. These figures also include the expected T_g of miscible blends as calculated from the Fox equation and show that the experimental single T_g values agree very well with the theoretical Fox equation in these same regions, suggesting that these systems do indeed exhibit miscibility in this window.

Last, phase-contrast optical microscopy was used to determine the temperature−composition phase diagrams of the three blends, LCPU/PS-*co*-VPh(10), LCPU/PS-*co*-VPh(20), and LCPU/PS-*co*-VPh(30), and are shown in Figure 16. There clearly is a miscibility window for these three systems, which demonstrates that the presence of significant hydrogen bonding can indeed induce miscibility in a rod/coil polymer blend. Moreover, comparison of the miscibility windows of these three systems shows that the system with the optimized extent of intermolecular hydrogen bonding (LCPU/ PS-*co*-VPh(20)) also is the system with the largest miscibility window. Clearly, these results demonstrate that optimizing the extent of intermolecular hydrogen bonding between two polymers will provide the best opportunity to induce miscibility in a polymer blend. Moreover, these and other recent results suggest that this optimal amount of intermolecular hydrogen bonding can be attained when the hydrogen-bonding moieties are sufficiently separated along the polymer chain.

Thus, these results provide guidelines by which true molecular composites, i.e., miscible blends of a liquid crystalline polymer and an amorphous polymer, can be designed and reproducibly created. This is accomplished by mixing a LCP with an amorphous polymer that has been modified to include well-separated functional groups that can form strong intermolecular interactions with the LCP. It is worth emphasizing that this separation of hydrogen-bonding moieties means that the functional group is present as a minor component in the amorphous copolymer, and thus the modification of the amorphous polymer (and its properties) is minimal.

Conclusion

The results of this study demonstrate that it is possible to create a true molecular composite by inducing miscibility in a blend containing a liquid crystalline polymer and an amorphous polymer by slightly modifying the amorphous polymer to promote hydrogen bonding between the two polymers. The results show that, by optimizing the extent of hydrogen bonding between the two blend components, the broadest miscibility window in the phase diagram is found. Furthermore, this optimization occurs when the hydrogen-bonding functional groups are separated along the polymer chain, a parameter that can be controlled by varying the composition of the amorphous copolymer. Improvement of the rotational freedom of the functional groups with increased spacing contributes to this trend. Also important is the decrease in the probability of intramolecular H bonding with an increase in the distance between O−H groups, which improves the probability that a given O−H group can participate in intermolecular H bonding.

Acknowledgment. The authors thank the National Science Foundation, Division of Materials Research, for financial support (CAREER-DMR-9702313) which funded this research.

References and Notes

(1) Wissburn, K. F. *J. Rheol. (N.Y.)* **1981**, *25* (6), 619.
(2) Wissburn, K. F.; Griffin, A. C. *J. Polym. Sci., Polym. Phys. Ed.* **1982**, *20*, 1835.
(3) Wissburn, K. F. *Br. Polym. J.* **1980**, *12*, 163.
(4) Cogswell, F. N. *Br. Polym. J.* **1980**, *12*, 170.
(5) Prasadarao, M.; Pearce, E. M.; Han, C. N. *J. Appl. Polym. Sci.* **1982**, *27*, 1343.
(6) Takayanagi, M.; Ogata, T.; Morikawa, M.; Kai, T. *J. Macromol. Sci., Phys.* **1980**, *B17*, 591. Hwang, W. F.; Wiff, D. R.; Verschoore, C.; Price, G. E.; Helminiak, T. E.; Adams, W. W. *Polym. Eng. Sci.* **1983**, *23*, 784. Hwang, W. F.; Wiff, D. F.; Benner, C.; Helminiak, T. E. *J. Macromol. Sci., Phys.* **1983**, *B22* (2), 231.
(7) Pawlikowski, G. T.; Dutta, D.; Weiss, R. A. *Annu. Rev. Mater. Sci.* **1991**, *21*, 159.
(8) Painter, P. C.; Tang, W. L.; Graf, J. F.; Thomson, B.; Coleman, M. M. *Macromolecules* **1991**, *24*, 3929.
(9) Stein, R. S.; Sethumadhavan, M.; Gaudhania, R. A.; Adams, T.; Guarrera, D.; Roy, S. K. *Pure Appl. Chem.* **1992**, *29*, 517. Cowie, J. M. G.; Nakata, S.; Adams, G. W. *Macromol. Symp.* **1996**, *112*, 207.
(10) Dadmun, M. D.; Han, C. C. *Mater. Res. Soc. Symp. Proc.* **1993**, *305*, 171.
(11) Tsou, L.; Sauer, J. A.; Hara, M. *Polymer* **2000**, *41*, 8103.
(12) Weiss, R. A.; Ghebremeskel, Y.; Charbonneau, L. *Polymer* **2000**, *41*, 3471.
(13) Flory, P. J. *Principles of Polymer Chemistry;* Cornell University Press: Ithaca, NY, 1953.
(14) Flory, P. J. *J. Chem. Phys.* **1942**, *10*, 51.
(15) Huggins, M. L. *J. Am. Chem. Soc.* **1942**, *64*, 1712.
(16) Flory, P. J. *Macromolecules* **1978**, *11*, 1138.
(17) Flory, P. J. *J. Am. Chem. Soc.* **1965**, *87*, 1833.
(18) Coleman, M. M.; Graf, J. F.; Painter, P. C. *Specific Interactions and the Miscibility of Polymer Blends;* Technomic Publishing Co.: Lancaster, PA, 1991.
(19) Painter, P. C.; Graf, J. F.; Coleman, M. M. *J. Chem. Phys.* **1990**, *10*, 6166.
(20) Vetysmann, B. A.; Painter, P. C. *J. Chem. Phys.* **1993**, *99*, 9272.
(21) Coleman, M. M.; Painter, P. C. *Prog. Polym. Sci.* **1995**, *20*, 1.
(22) Coleman, M. M.; Pehlert, G. J.; Painter, P. C. *Macromolecules* **1996**, *29*, 6820.
(23) Pehlert, G. H.; Painter, P. C.; Veytsman, B.; Coleman, M. M. *Macromolecules* **1997**, *30*, 3671.
(24) Hu, Y.; Painter, P. C.; Coleman, M. M. *Macromolecules* **1998**, *31*, 3394.
(25) Pehlert, G. H.; Painter, P. C.; Coleman, M. M. *Macromolecules* **1998**, *31*, 8423.
(26) Radmard, B.; Dadmun, M. D. *Polymer* **2001**, *42*, 1591.
(27) Painter, P. C.; Veytsman, B.; Kumar, S.; Shenoy, S.; Graf, J. F.; Xu, Y.; Coleman, M. M. *Macromolecules* **1997**, *30*, 932.
(28) Painter, P. C.; Berg, L. P.; Veytsman, B.; Coleman, M. M. *Macromolecules* **1997**, *30*, 7529.
(29) Pruthtikul, R.; Painter, P. C.; Coleman, M. M.; Tan, N. R. *Macromolecules*, in press.
(30) Tang, W. L.; Coleman, M. M.; Painter, P. C. *Macromol. Symp.* **1994**, *84*, 315.
(31) Khatri, C. A.; Vaidya, M. M.; Levon, K.; Jha, S. K.; Green, M. M. *Macromolecules* **1995**, *28*, 4719.
(32) Stenhouse, P. J.; Valles, E. M.; Kantor, S. W.; MacKnight, W. J. *Macromolecules* **1989**, *22*, 1467.
(33) Coleman, M. M.; Lee, K. H.; Skrovanek, D. J.; Painter, P. C. *Macromolecules* **1986**, *19*, 2149.
(34) Radmard, B. Thesis, The University of Tennessee, Knoxville, Dec 1999.
(35) Coleman, M. M.; Painter, P. C. *Fundamentals of Polymer Science*, 2nd ed.; Technomic Publishing Co.: Lancaster, PA, 1997.
(36) Dean, L.; Brisson, J. *Polymer* **1998**, *39*, 793.
(37) Lee, J. Y.; Painter, P. C.; Coleman, M. M. *Macromolecules* **1988**, *21*, 346.

MA011031X